

# The Effect of Mechanical Stress on Ligamentum Flavum Hypertrophy; Utilization of Novel In Vitro Multi-torsional Stretch Loading Device

**Woo-Keun Kwon**

Department of Neurosurgery, Korea University Guro Hospital, Korea University College of Medicine, Seoul, Korea

**Chang Hwa Ham**

Department of Neurosurgery, Korea University Guro Hospital, Korea University College of Medicine, Seoul, Korea

**Hyuk Choi**

Department of Medical Sciences, Graduate School of Medicine, Korea University, Seoul, Korea

**Seung Min Baek**

Department of Medical Sciences, Graduate School of Medicine, Korea University, Seoul, Korea

**Jae Won Lee**

Department of Medical Sciences, Graduate School of Medicine, Korea University, Seoul, Korea

**Youn-Kwan Park**

Department of Neurosurgery, Korea University Guro Hospital, Korea University College of Medicine, Seoul, Korea

**Hong Joo Moon**

Department of Neurosurgery, Korea University Guro Hospital, Korea University College of Medicine, Seoul, Korea

**Joo Han Kim** (✉ [nskjh94@gmail.com](mailto:nskjh94@gmail.com))

Department of Neurosurgery, Korea University Guro Hospital, Korea University College of Medicine, Seoul, Korea

---

## Research Article

**Keywords:** Ligamentum flavum, hypertrophy, spinal stenosis, mechanical stretching, MMP, inflammation

**Posted Date:** June 22nd, 2021

**DOI:** <https://doi.org/10.21203/rs.3.rs-635210/v1>

**License:** © ⓘ This work is licensed under a Creative Commons Attribution 4.0 International License.

[Read Full License](#)

# Abstract

## *Objective*

We developed a novel multi-torsional mechanical stretch stress (MSS) loading device for ligamentum flavum (LF) cells and evaluated its influence on the development of ligamentum flavum hypertrophy (LFH), a common cause of lumbar spinal canal stenosis.

## *Materials and Methods*

Stretch strength of the device was optimized by applying 5% and 15% MSS loads for 24, 48, and 72 h. A cytotoxicity assay of human LF cells was performed and the results were compared to control (0%) MSS. Inflammatory markers (interleukin [IL]-6, IL-8), vascular endothelial growth factor [VEGF], and extracellular matrix (ECM)-regulating cytokines (matrix metalloproteinase [MMP]-1, MMP-3 and MMP-9, and tissue inhibitor of metalloproteinase [TIMP]-1 and TIMP-2) were quantified via enzyme-linked immunosorbent assay.

## *Results*

Using our multi-torsional MSS loading device, 5% MSS for 24 h was optimal for LF cells. Under this condition, the IL-6 and IL-8 levels, VEGF level, and MMP-1, MMP-3, and TIMP-2 were significantly increased, compared to the control.

## *Conclusion*

Using the novel multi-torsional MSS loading device we confirmed that, mechanical stress enhances the production of inflammatory cytokines and angiogenic factors, and altered the expression of ECM-regulating enzymes, possibly triggering LFH. This discovery enhances our understating of the effects of mechanical stress on LFH.

# Introduction

Up to 70% of the general population experiences chronic lower back pain (LBP) once or more throughout their lifetime.<sup>1</sup> Among the many possible causes of chronic LBP, the prevalence of lumbar spinal canal stenosis (LSCS) in the elderly population is gradually increasing.<sup>2</sup> LSCS is also associated with lower-extremity radiculopathy and neurogenic claudication, which greatly affects the walking distance of the elderly. These clinical symptoms are associated with daily quality of life and therefore are of great interest to spinal physicians. The pathomechanism of LSCS is unclear, but facet joint enlargement, central intervertebral disc bulging, and ligamentum flavum hypertrophy (LFH) are contributing factors.<sup>3</sup> Among them, LFH secondary to the aging process or mechanical stimulation induced by instability of the spinal segment are key.<sup>4</sup> Therefore, research on the physiologic basis of LFH has caught the attention of

spinal specialists, who agree that inflammation, angiogenesis, and matrix regulation of ligamentum flavum influence the development of LFH.<sup>5-9</sup>

Mechanical stress on the ligamentum flavum is a major contributing factor to LFH. Hayashi *et al.* reported that mechanical stress concentration was directly linked to LFH in a rabbit model,<sup>10,11</sup> and Hur *et al.* emphasized the link between angiogenesis and mechanical stress-induced LFH.<sup>7</sup> Other studies have revealed an association between inflammation triggered by mechanical stress and LFH.<sup>6-9</sup> Nonetheless, it is doubtful whether these studies mimic *in vivo* mechanical stress. In this study, we developed a novel multi-torsional cell plate stretch device that mimics *in vivo* mechanical stress on ligamentum flavum tissue. We evaluated the molecular biological responses related to inflammation, angiogenesis, and extracellular matrix (ECM) regulation of ligamentum flavum cells to various stress loads to identify the stress load that best mimics LFH.

## Results

### Optimizing MSS Load on LF Cells

Using dual-step motor generators controlled by motor drivers, multi-torsional MSS was successfully loaded on the assembled cell chambers (Video File Supplemental Data).

The tension-load was produced by optimizing the multi-torsional stretch strength and the cyclic load frequency, and 3D simulation was performed to visualize the expected load on the chambers (Fig. 4). Morphologic evaluation of LF cells by optical microscopy revealed no significant phenotypic change after 24 h of 5% MSS, whereas cell death was noted with more prolonged MSS loading.

### Cytotoxicity Assay of LF cells

Lactate dehydrogenase release from MSS loaded LF cells was measured to evaluate cytotoxicity at 24, 48, and 72 h after MSS loading. As presented in Fig. 5, MSS load on LF cells did not significantly affect LDH release at 5% stretch for 24 h, but at 15% stretch and exposure for 48 and 72 h LDH levels were significantly increased, indicating a cytotoxic effect.

### Effect of MSS Loading on Inflammatory Cytokines and Vascular Growth Factors

IL-6 and IL-8 release after MSS loading was  $296.80 \pm 89.35$  and  $72.27 \pm 11.12$  ng/mL, respectively, significantly higher than in the control group ( $174.97 \pm 58.12$  and  $56.43 \pm 5.59$  ng/mL, respectively). Furthermore, a significant increase in VEGF level following MSS loading ( $141.80 \pm 19.45$  ng/mL) was observed compared to the control group ( $23.97 \pm 8.16$  ng/mL) (Fig. 6, Table 1).

### Effect of MSS load on production of ECM-regulating factors

MMP-1, MMP-3, MMP-9, TIMP-1, and TIMP-2 release levels from LF cells loaded with MSS at 5% for 24 h were measured to assess ECM remodeling. Following MSS loading, MMP-1, MMP-3, and MMP-9 release levels were  $463.94 \pm 53.08$ ,  $579.92 \pm 90.43$ , and  $25.77 \pm 1.84$  ng/mL, respectively. The TIMP-2 release level was  $320.00 \pm 16.34$  ng/mL; TIMP-1 was undetectable. The MMP-1, MMP-3, and TIMP-2 release levels were significantly increased by MSS loading compared to the control group ( $330.15 \pm 35.41$ ,  $420.25 \pm 45.66$ , and  $273.87 \pm 16.40$  ng/mL, respectively) (Fig. 6, Table 1).

Table 1

Inflammatory Mediators, Angiogenic factor, and ECM-regulating Molecule Production from LF cells

Factors	Control	MSS load (5%, 24hrs)	p-value
IL-6	$174.97 \pm 58.12$	$296.80 \pm 89.35$	0.013*
IL-8	$56.43 \pm 5.59$	$72.27 \pm 11.12$	0.015*
VEGF	$23.97 \pm 8.16$	$141.80 \pm 19.45$	0.028*
MMP-1	$330.15 \pm 35.41$	$463.94 \pm 53.08$	0.049*
MMP-3	$420.25 \pm 45.66$	$579.92 \pm 90.43$	0.024*
TIMP-2	$273.87 \pm 16.40$	$320.00 \pm 16.34$	0.049*

**\* P < 0.05**

ECM, extracellular matrix; LF, Ligamentum Flavum; IL, interleukin; VEGF, vascular endothelial growth factor; MMP, matrix metalloproteinases; TIMP, tissue inhibitors of metalloproteinase;

Values unit; ng/mL.  $\pm$  SE

## Discussion

LSCS is of interest to spinal physicians due to its increasing prevalence and clinical significance. Prior reports have indicated that LFH and LSCS are significantly associated with various clinical symptoms including back pain and radiculopathy with or without neurogenic claudication.<sup>9,12-16</sup> The LF is a ligamentous structure lying over the dorsal aspect of the central spinal canal, LFH directly results in physical narrowing of the spinal canal leading to clinical LSCS. To discover a novel therapeutic candidate targeting LFH, it is important to understand the pathomechanism of LFH. Elucidating the role of mechanical stress on the LF is critical, and inflammation/angiogenesis of the LF following mechanical stress are hallmarks of LFH.

We previously reported that inflammation and subsequent angiogenesis are involved in the pathomechanism of LFH *in vitro*, indicative of close relationships among inflammation, angiogenesis, and LFH.<sup>6</sup> In a follow-up study of the association between *in vitro* and clinical data, we discovered links among mechanical stress, angiogenesis, and LFH.<sup>7</sup> However, these studies were limited in that mechanical stress was not loaded directly onto the LR cells. Instead, the effects of mechanical stress were evaluated indirectly based on radiological findings. In this study, we developed a novel mechanical stress loading device with multidirectional torsion that mimics the mechanical load on LF tissue *in vivo*. Rather than inducing inflammation by transforming growth factor- $\beta$ 1 (TGF- $\beta$ 1) or interleukin-1 $\beta$  (IL-1 $\beta$ ), we used mechanical stress on the LF and believe it reflects the effects of mechanical stress on LFH.

Our results demonstrated that multi-torsional MSS load for 24 h under 5% stretch force stimulation resulted in an increase in IL-6 and VEGF levels. IL-6 activates neutrophils, whose adhesion and fibrosis are promoted by increased expression of ECM-regulating molecules or cytokines.<sup>17</sup> A similar response leads to LFH after triggering inflammation in LF cells.<sup>6</sup> An increase in IL-6 can also upregulate mRNA expression and DNA synthesis of LF cells, resulting in ossification or fibrosis.<sup>18</sup> Our finding of a significant increase in IL-6 expression confirms that MSS loading induced inflammation in LF cells, mimicking the initial inflammatory phase of LFH. Likewise, VEGF initiates and stimulates the angiogenic cascade of LFH, and its concentration in degenerated or hypertrophied LF is significantly higher than that in healthy ligaments.<sup>6,7,19,20</sup> MSS stimulation for 24 h resulted in marked elevation of VEGF expression in LF cells, indicating that MSS loading mimics the angiogenic cascade that occurs after an inflammatory reaction.

As well as inflammation and angiogenesis, the resultant changes in ECM-modulating factors (such as the elastin to collagen ratio) are important. Our data on ECM-regulating enzymes provide insight into the response of LF cells to mechanical stress. MMPs are endopeptidases involved in ECM homeostasis and in cell–cell interactions and angiogenesis. Significant changes or dysregulation of MMPs occur in cells during inflammation,<sup>21,22</sup> as well as in LF fibroblasts.<sup>8,23</sup> MMP-1 is a collagenase for all collagen subtypes, and MMP-3 a broad-spectrum proteinase that regulates activation of other MMPs.<sup>24</sup> Elevated MMP-1 and MMP-3 levels after MSS stimulation by our novel multi-torsional stress loading device are compatible with prior reports confirming an association with LFH.<sup>25,26</sup> This suggests the key role of mechanical stress in LFH as a result of altered ECM regulation in LF cells, indicating the dysregulation of regenerative potential and vulnerability to mechanical stress. However, Kim *et al.* reported increased expression of MMP-9 after inflammatory stimulation of LF cells *in vitro*,<sup>8</sup> and Lakemeier *et al.* indicated that MMP-9 expression is higher in LFH tissue.<sup>19</sup> TIMPs also regulate ECM homeostasis, and TIMP-1 and TIMP-2 play key roles in fibrosis in various cell types by increasing proliferation. Park *et al.* hypothesized that TIMP-1 and TIMP-2 influence LFH by increasing ECM density and promoting hypertrophy by suppressing MMP activities.<sup>4</sup> This hypothesis was confirmed by the significant association between elevated TIMP-1 and TIMP-2 expression in LF fibroblasts and spinal stenosis, a reproducible finding of

several different experiments of various methods.<sup>27</sup> This is compatible with our TIMP-1 and TIMP-2 expression data.

Mechanical stress is a key factor in LFH, as confirmed by *in vitro*<sup>28–32</sup>, *in vivo*<sup>10,11</sup>, and clinical studies<sup>7</sup>. Chao *et al.* developed an *in vitro* method of loading stress on LF cells by centrifuging them in a horizontal microplate rotor.<sup>32</sup> Nakamura *et al.* loaded a cyclic uniaxial load to LF cells by attaching the cell culture chamber to a stretching apparatus,<sup>28</sup> and Nakatani *et al.* loaded mechanical stress using a vacuum unit to pull a flexible cell culture plate from the center.<sup>30</sup> It is meaningful that centrifugal and cyclic one-dimensional mechanical forces on LF fibroblasts affected the mechanostress pathway. However, because one- and two-dimensional forces are unlike that on LF tissue *in vivo*, the accuracy of the model is unknown. Therefore, it is significant that we developed a reproducible repetitive mechanical stress loading device that recapitulates the mechanical stress on LF cells. The device will be used to provide insight into the role of direct mechanical stress on LFH *in vitro* and the cells' fate after mechanical stress loading.

## Materials And Methods

### Ethic declaration

This study was reviewed and approved by the local ethics committee (Research Ethics Committee of Korea University Guro Hospital: approval number K2017-0991) and has been performed in accordance with the ethical standards as laid down in the 1964 Declaration of Helsinki and its later amendments. Informed consent was obtained from all participants.

### Human LF Cell Isolation and Culture

This study was approved by the Institutional Review Board (IRB) of our institute. Human LF tissues were collected during surgeries on the lumbar spine for herniated nucleus pulposus, following the regulations of the IRB. LF cells were isolated from the tissues of five patients of normal LF thickness. LF tissues harvested in the operating room were placed in sterile Ham's F-12 medium (Gibco-BRL, Grand Island, NY) containing 1% penicillin/streptomycin (P/S; Gibco-BRL) and 5% fetal bovine serum (FBS; Gibco-BRL). After a phosphate-buffered saline (PBS; Welgene, Gyeongsan-si, Gyeongsangbuk-do, Korea) wash, tissues were minced and digested for 1 h at 37°C in Dulbecco's modified Eagle's medium (DMEM; Welgene, Gyeongsan-si, Gyeongsangbuk-do, Korea) with 0.2% pronase (Calbiochem, La Jolla, CA). Next, LF tissues were incubated overnight at the same temperature in 0.025% collagenase I (Roche Diagnostics, Mannheim, Germany). LF cells were filtered through a sterile nylon-mesh cell strainer (pore size, 70 µm), centrifuged, and the pellets were resuspended and cultured in DMEM containing 10% FBS and 1% P/S in a humidified atmosphere of 5% CO<sub>2</sub> at 37°C. LF cultures were continued until reaching full confluence. The cells were trypsinized and replated for subculture. Subsequent experiments were conducted using these second-passage LF cells.

# Design and Implementation of the Novel Mechanical Stretch Stress Loading System

We fabricated a multiple-multidirectional mechanical stretch stress (MSS) loading chamber system capable of incubating dishes containing LF cells. The multi-torsional cell plate stretch device comprises a roofless metal frame containing fixation panels, twisting parts, culture chambers, and a controller. Multiple chambers are seated parallel on the fixation panel facing upwards (Fig. 1). The sides of the chamber are fixated to two separate and parallel-oriented fixation panels, which pulls the chamber by moving in the opposite direction. In addition, the fixation panels are coupled to the twisting part to produce torsion stress on multiple chambers. The parallel chambers are aligned and stretched in the same direction and with identical power simultaneously. Each chamber is made of flexible polydimethylsiloxane (PDMS) by photolithography, that can contain cell cultures and stretch or twist. An optically transparent, ultrathin (100  $\mu\text{m}$ ) membrane was applied to the well bottom to render the stretch chambers compatible with optical and fluorescence microscopy (Fig. 2). The MSS force developed by two step motor generators were controlled by Arduino Uno and L293D motor drivers, regulating the strength of the stretch and torsional stress. The optimal cyclic directions and loading were established after multiple virtual simulations. A 4-degree tilt away from the panel provides 2 mm stretch and 3 mm sliding of each panel beneath the chambers, resulting a in 10 degree of rotation tilt of the chamber corners and torsional stretch on the PDMS chambers (Fig. 3). The PDMS chambers are designed to be assembled on the MSS device after cell attachment has been confirmed. In addition, to determine the expected stretch load force on the internal surface of the chamber, a three-dimensional (3D) simulation program (Inventor, Autodesk Inc, CA) was used. The torsional stress loaded on the external chamber surface was analyzed and presented as stress-strain ratios.

## Mechanical Stretch Stress Loading on LF cells

LF cells were plated on the PDMS chamber at a density of  $1.0 \cdot 10^4$  /mL. After 24 h of incubation, cell attachment to the cell chamber wall was verified, and the cells were subjected to MSS. Multi-torsional MSSs of 0% (no stretch–control), 5%, and 15% of maximal stretch load were applied to multiple cell plate chambers simultaneously.

## Enzyme-Linked Immunosorbent Assay

Concentrations of vascular growth factor (VEGF), interleukin (IL)-6 and IL-8, matrix metalloproteinase (MMP)-1 and MMP-3, and tissue inhibitor of metalloproteinase (TIMP)-1 and TIMP-2 were analyzed by ELISA using commercially available kits (R&D Systems, Minneapolis, MN) following the manufacturer's recommended protocols. All experiments were conducted in duplicate.

## Statistical Analysis

Data are means  $\pm$  standard deviations (SDs) for individual experiments using independent cell cultures. P values were calculated using Student's *t*-test or the Mann–Whitney U test, as appropriate according to

sample size and distribution normality. P-values < 0.05 were considered to indicate statistical significance.

## Declarations

## Author contributions

KWK, HCH equally assisted with study design, data collection, data interpretation, and drafting of the manuscript. CH, BSM, LJW, PYK, MHJ assisted with study design, data collection, data interpretation, KJH is the corresponding author and assisted with study design, data collection, data interpretation and drafting of the manuscript as well.

## Competing interests

This research was supported by Basic Science Research Program through the National Research Foundation of Korea(NRF) funded by the Ministry of Education (NRF-2017R1D1A1B03029729)

## References

1. Andersson, G. B. Epidemiological features of chronic low-back pain. *Lancet* **354**, 581-585, doi:10.1016/S0140-6736(99)01312-4 (1999).
2. Kalichman, L. *et al.* Spinal stenosis prevalence and association with symptoms: the Framingham Study. *Spine J* **9**, 545-550, doi:10.1016/j.spinee.2009.03.005 (2009).
3. Szpalski, M. & Gunzburg, R. Lumbar spinal stenosis in the elderly: an overview. *Eur Spine J* **12 Suppl 2**, S170-175, doi:10.1007/s00586-003-0612-1 (2003).
4. Park, J. B., Lee, J. K., Park, S. J. & Riew, K. D. Hypertrophy of ligamentum flavum in lumbar spinal stenosis associated with increased proteinase inhibitor concentration. *J Bone Joint Surg Am* **87**, 2750-2757, doi:10.2106/JBJS.E.00251 (2005).
5. Hur, J. W. *et al.* Myofibroblast in the ligamentum flavum hypertrophic activity. *Eur Spine J* **26**, 2021-2030, doi:10.1007/s00586-017-4981-2 (2017).
6. Moon, H. J. *et al.* The angiogenic capacity from ligamentum flavum subsequent to inflammation: a critical component of the pathomechanism of hypertrophy. *Spine (Phila Pa 1976)* **37**, E147-155, doi:10.1097/BRS.0b013e3182269b19 (2012).
7. Hur, J. W. *et al.* The Mechanism of Ligamentum Flavum Hypertrophy: Introducing Angiogenesis as a Critical Link That Couples Mechanical Stress and Hypertrophy. *Neurosurgery* **77**, 274-281; discussion 281-272, doi:10.1227/NEU.0000000000000755 (2015).
8. Kim, B. J. *et al.* Expression of matrix metalloproteinase-2 and -9 in human ligamentum flavum cells treated with tumor necrosis factor-alpha and interleukin-1beta. *J Neurosurg Spine* **24**, 428-435, doi:10.3171/2015.6.SPINE141271 (2016).

9. Sairyo, K. *et al.* Pathomechanism of ligamentum flavum hypertrophy: a multidisciplinary investigation based on clinical, biomechanical, histologic, and biologic assessments. *Spine (Phila Pa 1976)* **30**, 2649-2656 (2005).
10. Hayashi, K. *et al.* Mechanical stress induces elastic fibre disruption and cartilage matrix increase in ligamentum flavum. *Sci Rep* **7**, 13092, doi:10.1038/s41598-017-13360-w (2017).
11. Hayashi, K. *et al.* Fibroblast Growth Factor 9 Is Upregulated Upon Intervertebral Mechanical Stress-Induced Ligamentum Flavum Hypertrophy in a Rabbit Model. *Spine (Phila Pa 1976)* **44**, E1172-E1180, doi:10.1097/BRS.0000000000003089 (2019).
12. Beamer, Y. B., Garner, J. T. & Shelden, C. H. Hypertrophied ligamentum flavum. Clinical and surgical significance. *Arch Surg* **106**, 289-292, doi:10.1001/archsurg.1973.01350150029008 (1973).
13. Park, J. B., Chang, H. & Lee, J. K. Quantitative analysis of transforming growth factor-beta 1 in ligamentum flavum of lumbar spinal stenosis and disc herniation. *Spine (Phila Pa 1976)* **26**, E492-495 (2001).
14. Towne, E. B. & Reichert, F. L. Compression of the Lumbosacral Roots of the Spinal Cord by Thickened Ligamenta Flava. *Ann Surg* **94**, 327-336, doi:10.1097/00000658-193109000-00002 (1931).
15. Okuda, T. *et al.* The pathology of ligamentum flavum in degenerative lumbar disease. *Spine (Phila Pa 1976)* **29**, 1689-1697, doi:10.1097/01.brs.0000132510.25378.8c (2004).
16. Yoshida, M., Shima, K., Taniguchi, Y., Tamaki, T. & Tanaka, T. Hypertrophied ligamentum flavum in lumbar spinal canal stenosis. Pathogenesis and morphologic and immunohistochemical observation. *Spine (Phila Pa 1976)* **17**, 1353-1360, doi:10.1097/00007632-199211000-00015 (1992).
17. Romano, M. *et al.* Role of IL-6 and its soluble receptor in induction of chemokines and leukocyte recruitment. *Immunity* **6**, 315-325, doi:10.1016/s1074-7613(00)80334-9 (1997).
18. Park, J. O. *et al.* Inflammatory cytokines induce fibrosis and ossification of human ligamentum flavum cells. *J Spinal Disord Tech* **26**, E6-12, doi:10.1097/BSD.0b013e3182698501 (2013).
19. Lakemeier, S. *et al.* Expression of hypoxia-inducible factor-1alpha, vascular endothelial growth factor, and matrix metalloproteinases 1, 3, and 9 in hypertrophied ligamentum flavum. *J Spinal Disord Tech* **26**, 400-406, doi:10.1097/BSD.0b013e3182495b88 (2013).
20. Yayama, T. *et al.* Calcium pyrophosphate crystal deposition in the ligamentum flavum of degenerated lumbar spine: histopathological and immunohistological findings. *Clin Rheumatol* **27**, 597-604, doi:10.1007/s10067-007-0754-3 (2008).
21. Visse, R. & Nagase, H. Matrix metalloproteinases and tissue inhibitors of metalloproteinases: structure, function, and biochemistry. *Circ Res* **92**, 827-839, doi:10.1161/01.RES.0000070112.80711.3D (2003).
22. Parks, W. C., Wilson, C. L. & Lopez-Boado, Y. S. Matrix metalloproteinases as modulators of inflammation and innate immunity. *Nat Rev Immunol* **4**, 617-629, doi:10.1038/nri1418 (2004).
23. Warner, R. L. *et al.* Matrix metalloproteinases in acute inflammation: induction of MMP-3 and MMP-9 in fibroblasts and epithelial cells following exposure to pro-inflammatory mediators in vitro. *Exp Mol Pathol* **76**, 189-195, doi:10.1016/j.yexmp.2004.01.003 (2004).

24. Pasternak, B. & Aspenberg, P. Metalloproteinases and their inhibitors-diagnostic and therapeutic opportunities in orthopedics. *Acta Orthop* **80**, 693-703, doi:10.3109/17453670903448257 (2009).
25. Park, J. B., Kong, C. G., Suhl, K. H., Chang, E. D. & Riew, K. D. The increased expression of matrix metalloproteinases associated with elastin degradation and fibrosis of the ligamentum flavum in patients with lumbar spinal stenosis. *Clin Orthop Surg* **1**, 81-89, doi:10.4055/cios.2009.1.2.81 (2009).
26. Oh, I. S. & Ha, K. Y. Matrix metalloproteinase-3 on ligamentum flavum in degenerative lumbar spondylolisthesis. *Spine (Phila Pa 1976)* **34**, E552-557, doi:10.1097/BRS.0b013e3181aa0232 (2009).
27. Xu, Y. Q., Zhang, Z. H., Zheng, Y. F. & Feng, S. Q. MicroRNA-221 Regulates Hypertrophy of Ligamentum Flavum in Lumbar Spinal Stenosis by Targeting TIMP-2. *Spine (Phila Pa 1976)* **41**, 275-282, doi:10.1097/BRS.0000000000001226 (2016).
28. Nakamura, T. *et al.* Angiopoietin-like protein 2 induced by mechanical stress accelerates degeneration and hypertrophy of the ligamentum flavum in lumbar spinal canal stenosis. *PLoS One* **9**, e85542, doi:10.1371/journal.pone.0085542 (2014).
29. Nakamura, T. *et al.* Angiopoietin-like protein 2 promotes inflammatory conditions in the ligamentum flavum in the pathogenesis of lumbar spinal canal stenosis by activating interleukin-6 expression. *Eur Spine J* **24**, 2001-2009, doi:10.1007/s00586-015-3835-z (2015).
30. Nakatani, T. *et al.* Mechanical stretching force promotes collagen synthesis by cultured cells from human ligamentum flavum via transforming growth factor-beta1. *J Orthop Res* **20**, 1380-1386, doi:10.1016/S0736-0266(02)00046-3 (2002).
31. Cai, H. X. *et al.* Cyclic tensile strain facilitates the ossification of ligamentum flavum through beta-catenin signaling pathway: in vitro analysis. *Spine (Phila Pa 1976)* **37**, E639-646, doi:10.1097/BRS.0b013e318242a132 (2012).
32. Chao, Y. H., Tsuang, Y. H., Sun, J. S., Sun, M. G. & Chen, M. H. Centrifugal force induces human ligamentum flavum fibroblasts inflammation through activation of JNK and p38 pathways. *Connect Tissue Res* **53**, 422-429, doi:10.3109/03008207.2012.685132 (2012).

## Figures

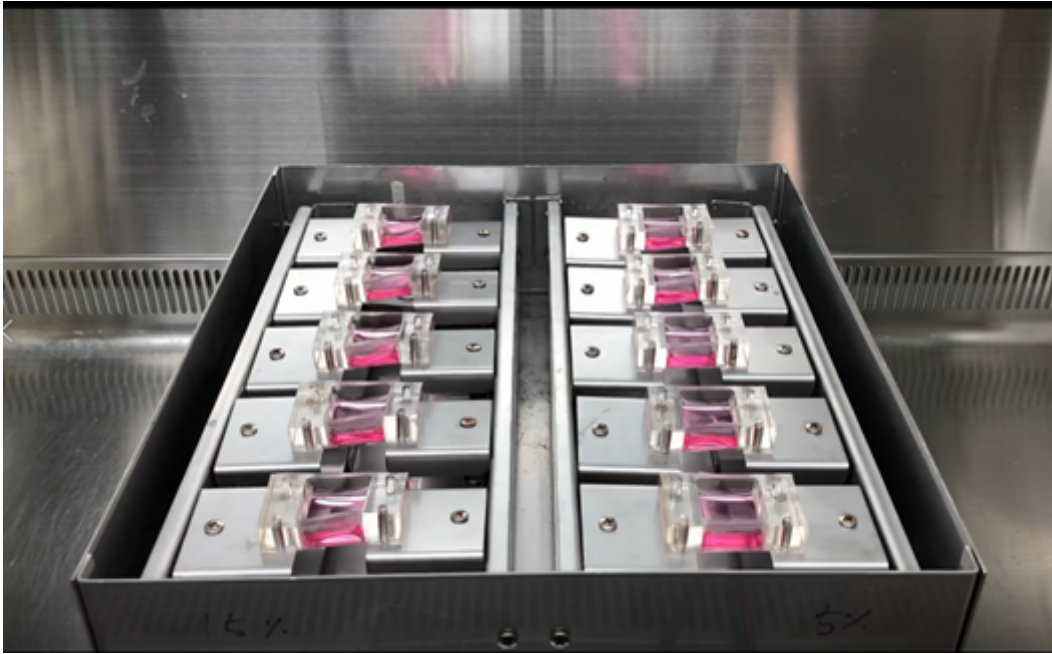


Figure 1

An open metal frame with multiple chambers seated parallel to the fixation panels.

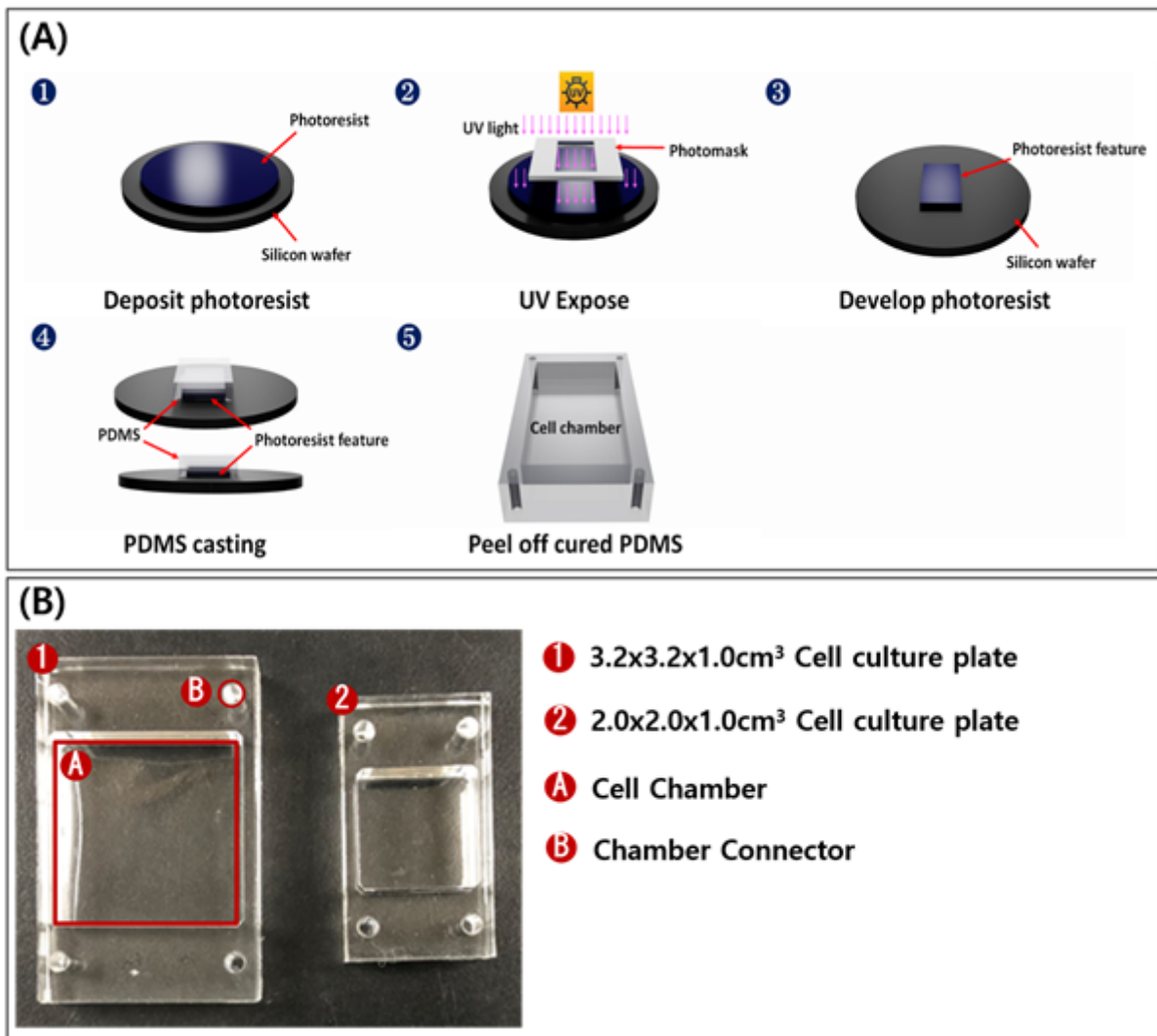


Figure 2

(A) Photolithography process; (B) PDMS stretch chambers compatible with the panels.

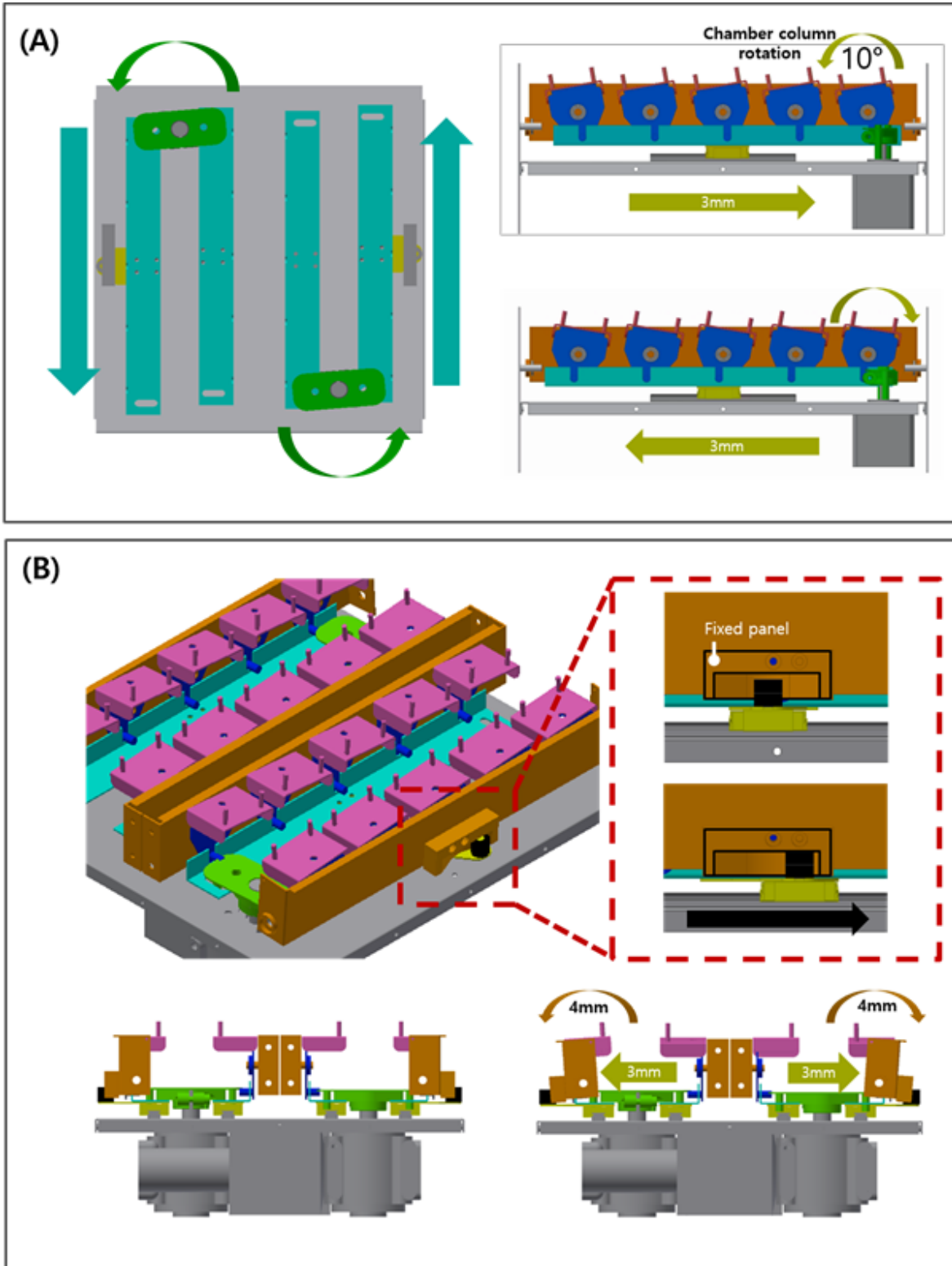
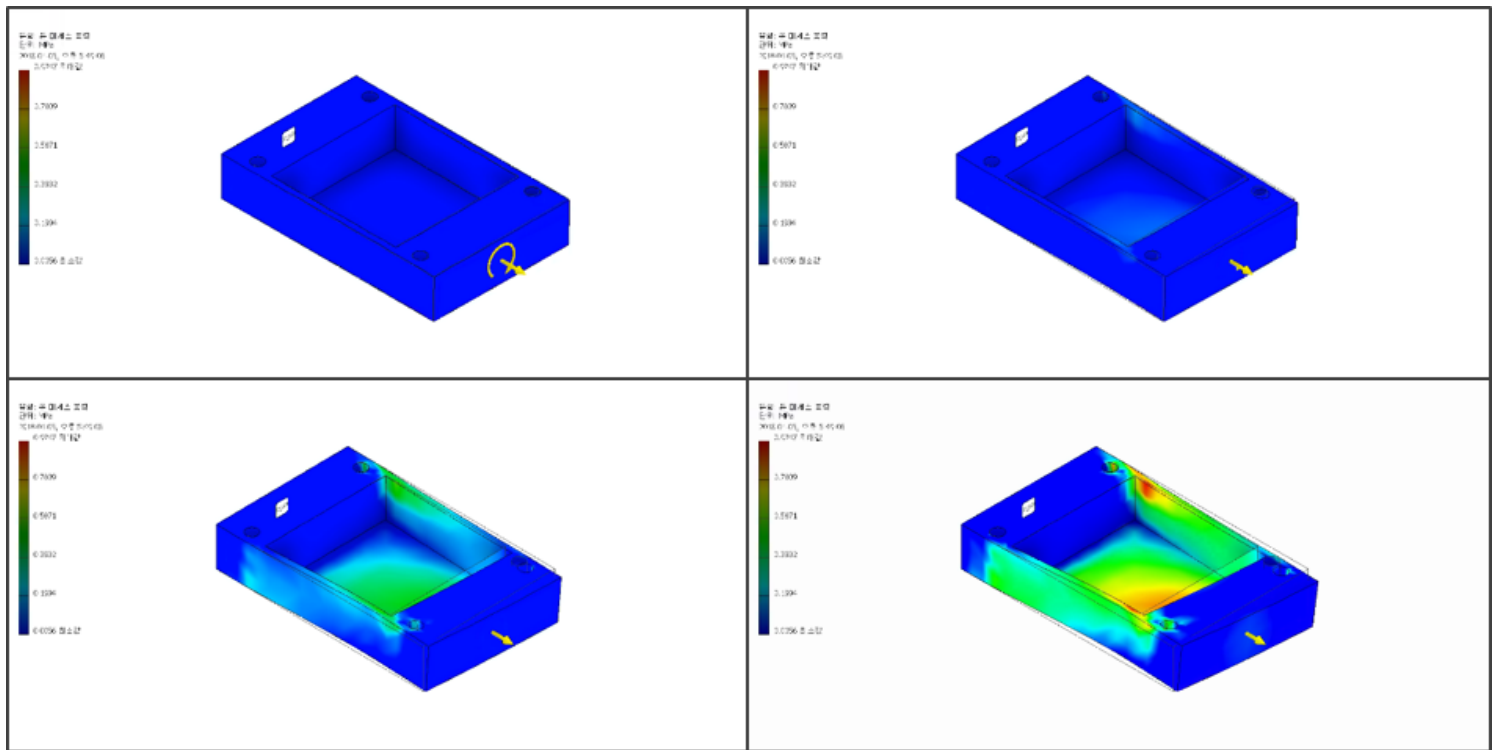


Figure 3

Two-step motor generators; (A) Producing a 10-degree rotational tilt of the chamber corners with resultant torsional stretch on the PDMS chambers (B) 4-degree tilt away from the panel results in 2 mm stretch and

3 mm sliding of each panel beneath the chambers



**Figure 4**

Three-dimensional simulation of the expected load on the chambers. The torsional stress loaded on the external chamber surface is shown as the stress-strain ratio.

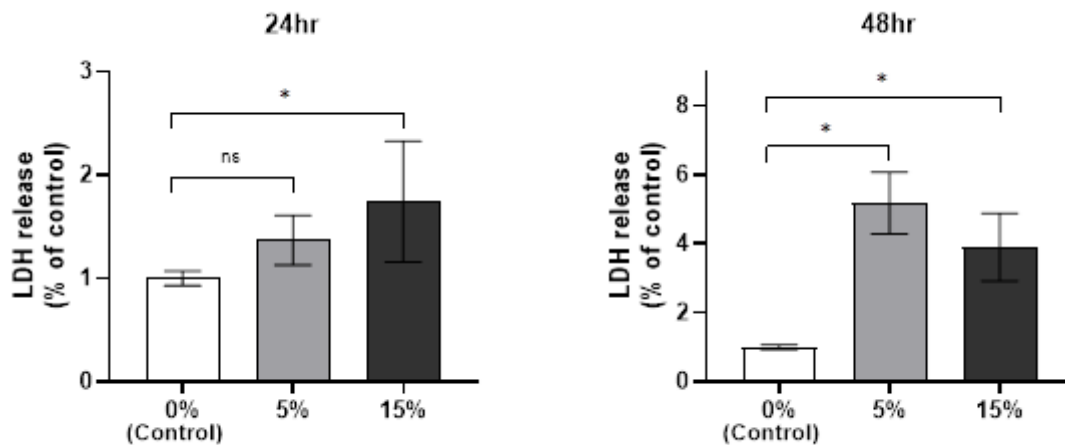


**Figure 5**

Cytotoxicity assay of ligamentum flavum cells. MSS loading at 5% stretch for 24 h on ligamentum flavum cells did not significantly affect the LDH release level. Stronger stretch (15%) and stretching for 48 h resulted in significantly increased LDH levels, indicating a cytotoxic effect.

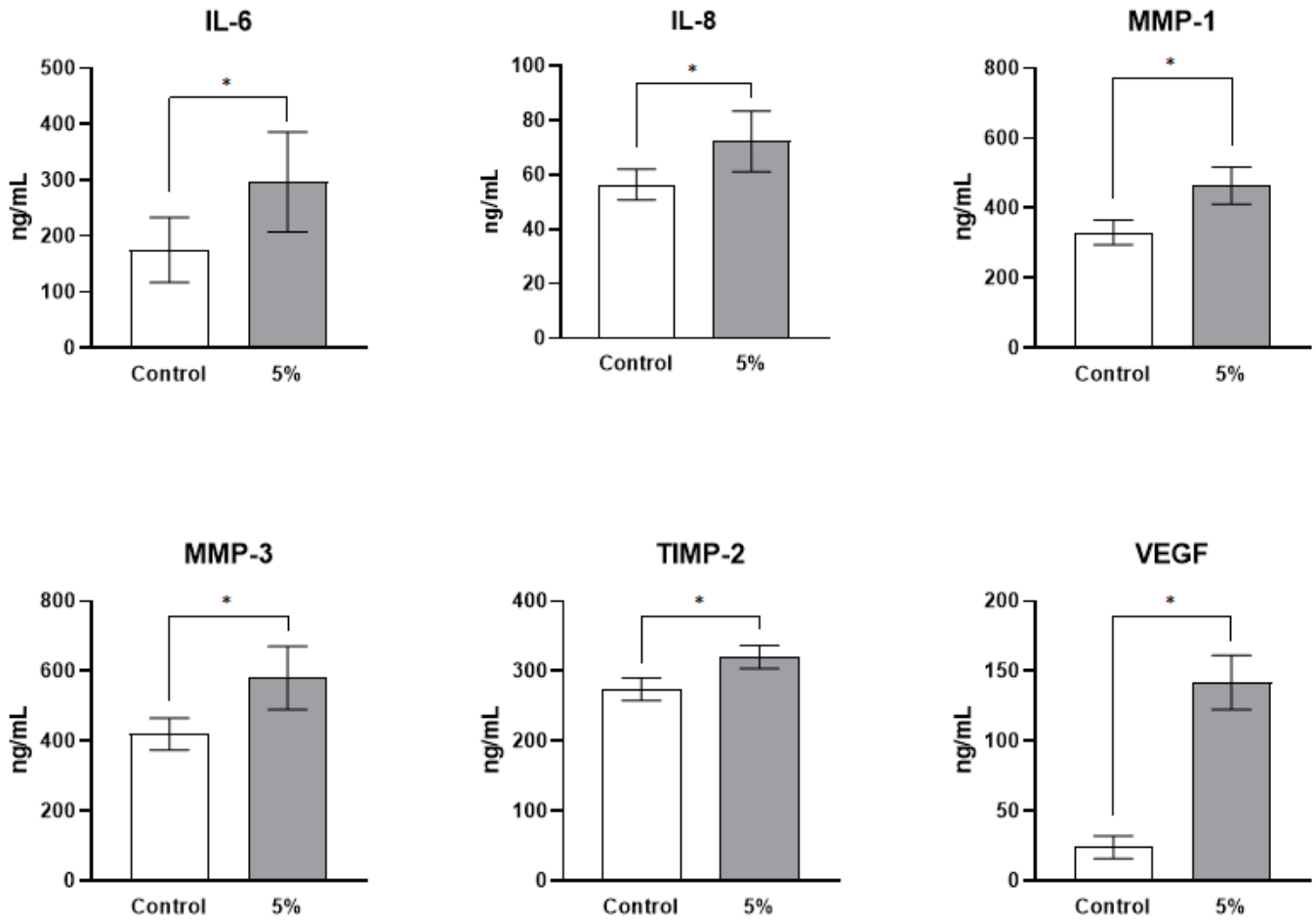


**Figure 6**

IL-6, IL-8, VEGF, MMP-1, MMP-3, and TIMP-2 release from ligamentum flavum cells loaded with MSS at 5% for 24 h was significantly increased compared to the control group.

## Supplementary Files

This is a list of supplementary files associated with this preprint. Click to download.

- [Device.mp4](#)